J. Mod. Transport. (2017) 25(1):52–57
DOI 10.1007/s40534-016-0120-8

www.springer.com/40534

Synthesis and photoelectrical performance of nanoscale PbS and Bi_2S_3 co-sensitized on TiO_2 nanotube arrays

Fanggong Cai[1,2] · Min Pan[1,2] · Yong Feng[2] · Guo Yan[2] · Yong Zhang[1] · Yong Zhao[1,3]

Received: 5 May 2016 / Revised: 13 October 2016 / Accepted: 20 October 2016 / Published online: 30 November 2016

Abstract TiO_2 films have been widely applied in photovoltaic conversion techniques. TiO_2 nanotube arrays (TiO_2 NAs) can be grown directly on the surface of metal Ti by the anodic oxidation method. Bi_2S_3 and PbS nanoparticles (NPs) were firstly co-sensitized on TiO_2 NAs (denoted as PbS/Bi_2S_3(n)/TiO_2 NAs) by a two-step process containing hydrothermal and sonication-assisted SILAR method. When the concentration of Bi^{3+} is 5 mmol/L, the best photoelectrical performance was obtained under simulated solar irradiation. The short-circuit photocurrent (J_{sc}) and photoconversion efficiency (η) of PbS/Bi_2S_3(5)/TiO_2 NAs electrode were 4.70 mA/cm and 1.13 %, respectively.

Keywords Solar cells · TiO_2 nanotube arrays · Bi_2S_3 · PbS · Surface photovoltage

1 Introduction

Industrial development and population growth have led to a surge in the global energy demands. Solar energy is an important source of renewable energy and has been widely applied in various fields including transport. Solar-powered cars [1] and aircrafts [2] depend on solar cells to convert sunlight into electricity to drive electric motors. In the future, they are expected to play a key role in reducing consumption of burning fossil fuels. Currently, crystalline silicon is the most common material used for solar cells. However, a large number of toxic substances are generated during the production of crystalline silicon.

Dye-sensitized solar cells (DSSCs) [3] have been well developed over the past two decades. With the advantages of facile preparation and low cost, nanoscale inorganic semiconductors are considered as ideal substitutes for organic dyes. Moreover, their band gaps can be conveniently tailored by controlling the size of nanoparticles [4]. PbS [5], Bi_2S_3 [6], and other inorganic semiconductors have been used to sensitize n-type wide-band gap semiconductor, such as TiO_2. TiO_2 nanotube arrays (TiO_2 NAs) are attracting considerable interest, because they can provide direct and efficient transport channels for photogenerated electrons, and promote the separation of photogenerated electrons and holes [7]. TiO_2 NAs can be grown directly on the surface of metal Ti by the anodic oxidation method [8]. Ti alloy with lightweight and high-strength is considered an ideal material for solar-powered cars and aircrafts. Therefore, we intend to sensitize TiO_2 NAs with inorganic semiconductors to construct solar cells, and study their photoelectric properties.

Previously, we had demonstrated that both Bi_2S_3 and PbS nanoparticles are efficient sensitizers for TiO_2 NAs [6, 9]. Nevertheless, the strategy of TiO_2 sensitized by the single inorganic semiconductor limited the further improvement of the photoelectric performance and light absorption property. As a result, co-sensitized strategy has been adopted by many researchers. On the other hand, it has been reported that the bulk nano-heterojunction

✉ Yong Zhao
yzhao@home.swjtu.edu.cn

[1] Superconductivity and New Energy R&D Center, Key Laboratory of Advanced Technology of Materials (Ministry of Education of China), Southwest Jiaotong University, Mail Stop 165#, Cheng du 610031, People's Republic of China

[2] National Engineering Labortary for Superconducting Materials, Western Superconducting Technologies Co. Ltd, Xi'an, People's Republic of China

[3] School of Physical Science and Technology, Southwest Jiaotong University, Chengdu 610031, People's Republic of China

structure formed by Bi_2S_3 and PbS quantum dots can enhance the carrier lifetime resulting from the separation of nanoscale phase, and then the photoelectric properties can be improved [10]. Thus, in this work, we first prepared PbS and Bi_2S_3 nanoparticles to co-sensitize TiO_2 NAs, and studied their photoelectric properties. The preparation process and photoelectric properties of PbS and Bi_2S_3 nanoparticles co-sensitized on TiO_2 NAs were discussed.

2 Methods

2.1 Preparation of TiO_2 NAs

An anodic oxidation method was used to grow TiO_2 NAs on the surface of Ti foil. In brief, Ti foil (3 cm × 1 cm × 0.25 mm) was anodized in ethylene glycol containing 0.25 wt% NH_4F at a constant voltage of 60 V for 6 h, while a larger Pt foil (3 cm × 4 cm) was used as the counter electrode. All experiments were carried out at room temperature. The as-prepared samples were annealed at 450 °C for 3.5 h.

2.2 Preparation of Bi_2S_3/TiO_2 NAs

Bi_2S_3 was deposited into anatase TiO_2 NAs by a hydrothermal method. At first, $Bi(NO_3)_3$ (100 mL) and $Na_2S_2O_3$ (100 mL) aqueous solutions with certain concentrations were prepared, respectively. The molar ratio of Bi^{3+} to $S_2O_3^{2-}$ was fixed at 2:3. In this work, three concentrations of Bi^{3+} were chosen, 1, 5, and 10 mmol L^{-1}. And then, both of $Bi(NO_3)_3$ and $Na_2S_2O_3$ aqueous solutions were mixed and stirred thoroughly to obtain precursor solution. The aforementioned precursor solution was transferred to a 25-mL Teflon-lined stainless steel autoclave containing anatase TiO_2 NAs sample. The autoclave was sealed and maintained at 100 °C for 24 h. The obtained sample is designated as $Bi_2S_3(n)/TiO_2$ NAs, where n represents the concentration of Bi^{3+}.

2.3 Preparation of $PbS/Bi_2S_3(n)/TiO_2$ NAs

PbS nanoparticles (PbS NPs) were attached to $Bi_2S_3(n)/TiO_2$ NAs using a sonication-assisted successive ionic layer adsorption and reaction (SILAR) method. In other words, the as-prepared $Bi_2S_3(n)/TiO_2$ NAs electrode was successively immersed into 5 mmol/L $Pb(NO_3)_2$ aqueous solution, D.I. water, 5 mmol L^{-1} Na_2S aqueous solution, and D.I. water again for 20 s each. According to our previous study [9], the SILAR cycles were carried out five times under ultrasonic waves of 20 kHz and 100 W to form PbS NPs of lower 4 nm. The sample was denoted as $PbS/Bi_2S_3(n)/TiO_2$ NAs.

2.4 Characterization

The morphologies and structure of all samples were examined using a field emission scanning electron microscope (FESEM, JSM 7001F, JEOL, Japan) and powder X-ray diffraction (XRD, PANalytical diffractometer), respectively. Energy dispersive X-ray analysis (EDX) attached to FESEM was used to qualitatively and quantitatively analyze the chemical composition of samples.

A surface photovoltage (SPV) measurement system was used to characterize the transport characteristics of photogenerated electron–holes pairs. For more details, please refer to Refs [6, 9, 11].

Photoelectric property of electrodes was studied using electrochemical work-station (Lanlike 2006A, China) in 0.5 mol/L Na_2S electrolyte. $PbS/Bi_2S_3(n)/TiO_2$ NA (on Ti foil) was used as the working electrode, while Pt foil and SCE were used as counter and reference electrode, respectively. The electrodes were tested under simulated sunlight at AM 1.5 (100 mW/cm^2) from a 500 W xenon lamp and an AM 1.5 filter. The effective surface area of the electrode was 1.0 × 1.5 cm for illumination.

3 Results and discussion

Previously, Bi_2S_3 NPs had successfully been deposited into TiO_2 NAs by hydrothermal method at 100 °C [6]. And PbS NPs also can be attached to TiO_2 NAs by a sonication-assisted SILAR method [9]. So, we believed that nanoscale Bi_2S_3 and PbS can be successively deposited on TiO_2 NAs using two methods mentioned above. Figure 1 shows the XRD pattern of $PbS/Bi_2S_3(1)/TiO_2$ NAs. Besides Ti and

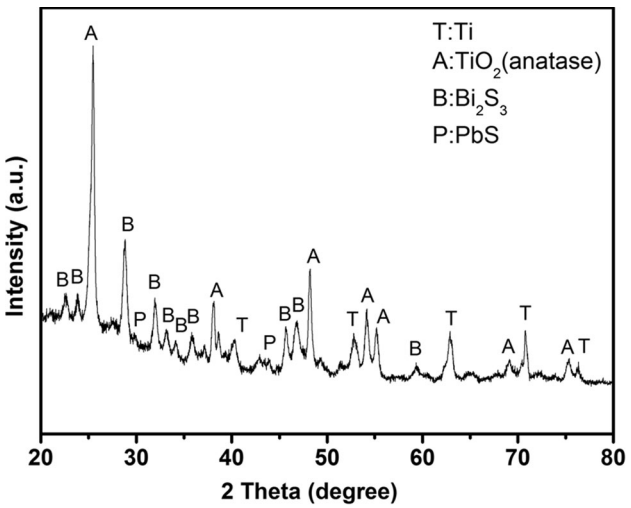

Fig. 1 XRD pattern of $PbS/Bi_2S_3(1)/TiO_2$ NAs. Symbols T, A, B, and P represent the peaks of metal Ti, anatase TiO_2, orthorhombic Bi_2S_3, and cubic PbS, respectively

anatase TiO_2, X-ray diffraction peaks of orthorhombic Bi_2S_3 and cubic PbS can also be found. Symbols T, A, B, and P in Fig. 1 represent the peaks of Ti, TiO_2, Bi_2S_3, and PbS, respectively. The XRD result confirms that PbS/Bi_2S_3(n)/TiO_2 NAs composite can be formed.

Figure 2 shows the typical top-view FESEM images of pure TiO_2 NAs and PbS/Bi_2S_3(n)/TiO_2 NAs. The regularly arranged TiO_2 NAs fabricated by anodic oxidation are shown in Fig. 2a; its diameter and wall thickness are about 140 and 20 nm, respectively. The views of PbS/Bi_2S_3(n)/TiO_2 NAs (Fig. 2b, c, and d) illustrate that some nanoparticles are decorated into TiO_2 nanotubes, including interior of nanotubes and outside of nanotube walls. According to the XRD result, we confirm that these nanomaterials are Bi_2S_3 and PbS. The filling degrees of TiO_2 NAs increased along with the concentration of Bi^{3+}. We assume that the content of PbS in all samples remains unchanged, because PbS NPs were synthesized using the same conditions. The content of Bi_2S_3 in TiO_2 NAs was determined by EDX experiments, as shown in Fig. 3. The results of EDX analysis show that the mass fractions of the Bi element are 4.18 %, 14.24 %, and 30.36 % with respect to that of PbS/Bi_2S_3(n)/TiO_2 NAs, respectively for $n = 1$, 5, and 10.

TiO_2 is an important n-type semiconductor with a wide-band gap ($E_g = 3.2$ eV), while n-type Bi_2S_3 has a narrow

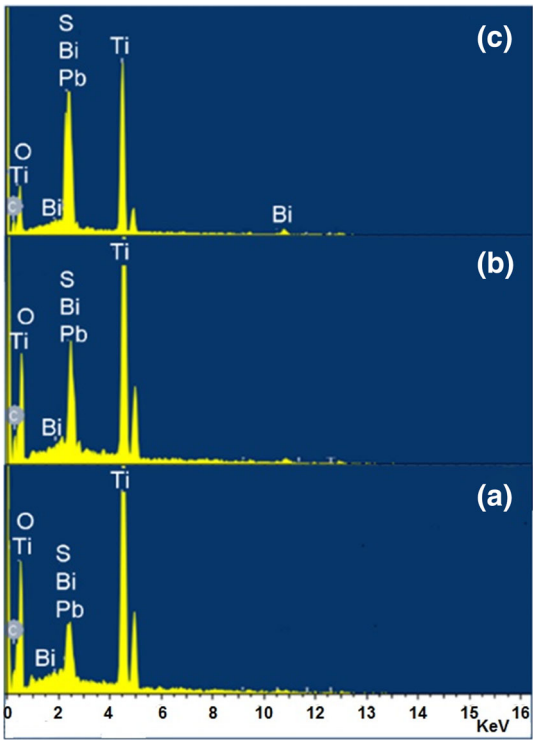

Fig. 3 EDX spectra of PbS/Bi_2S_3(n)/TiO_2 NAs. a, b, and c for $n = 1$, 5, and 10, respectively

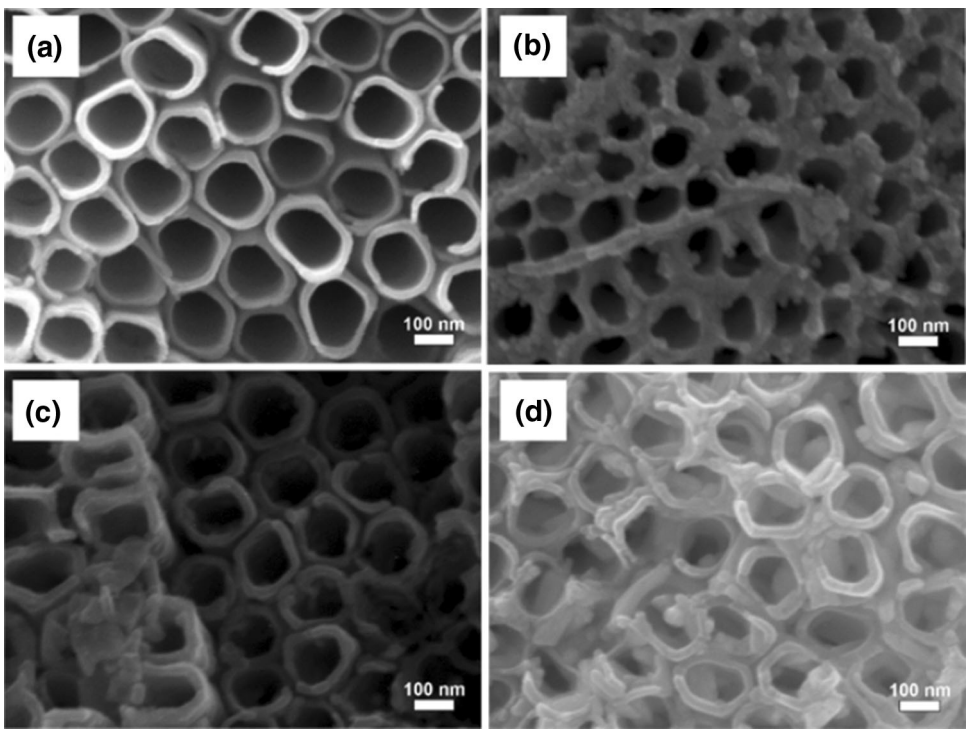

Fig. 2 FESEM images: *top-view* of **a** pure TiO_2 NAs and **b**, **c**, and **d** PbS/Bi_2S_3(n)/TiO_2 NAs composites ($n = 1$, 5, and 10, respectively)

E_g of 1.3 eV. Photogenerated electrons can easily transfer from the Bi_2S_3 surface to TiO_2, because Bi_2S_3 has a more negative conduction band (CB) [12]. The E_g of bulk PbS is only 0.41 eV, but is directly dependent on the size of nanoparticles. According to Refs. [13] and [14], PbS NPs of 4 nm or lower has a more negative CB than that of TiO_2. Previously, we found that PbS NPs (<4 nm) can be fabricated using a sonication-assisted SILAR method when cycle number (n) is 5 [9]. Figure 4a schematically illustrates energy band diagram of PbS, Bi_2S_3, and TiO_2. Thus, we hope to construct PbS/Bi_2S_3/TiO_2 NAs heterojunction to promote the separation and transport of photogenerated electron–hole pairs.

SPV system is an effective tool to investigate the behavior of photogenerated charge carriers. SPV spectra of PbS/Bi_2S_3(n)/TiO_2 NAs are shown in Fig. 5. Simultaneously, corresponding SPV spectrum of pure Bi_2S_3 is shown in the inset of Fig. 5. The signal of SPV is due to the difference of surface potential barriers before and after light illumination [15]. Noticeable SPV response ranging from 300 to 400 nm is found for TiO_2 NAs attributed to its wide E_g. For pure Bi_2S_3, it has a strong response in the whole-tested wave spectrum, especially 400–800 nm, because Bi_2S_3 has a narrow E_g (1.3 eV). The SPV response of PbS/Bi_2S_3(n)/TiO_2 NAs increases gradually with the amount of Bi_2S_3 in the range over 400 nm. This is because SPV response is directly related to the amount of semiconductor. However, in the range of 300–400 nm, PbS/Bi_2S_3(5)/TiO_2 NAs has strongest SPV response intensity in all PbS/Bi_2S_3(n)/TiO_2 NAs. This result suggests that there is one or more heterojunction among PbS, Bi_2S_3, and TiO_2 NAs, which aids the separation of photogenerated electrons and holes. Both Bi_2S_3 and TiO_2 are n-type semiconductors, the direction of an internal electric field in Bi_2S_3 (n)/TiO_2 heterojunction is opposite to that of built-in electric field in p-type PbS. Thus, when PbS NPs are coupled with Bi_2S_3(n)/TiO_2 NAs, the SPV response in 300–400 nm spectral range appears to decline.

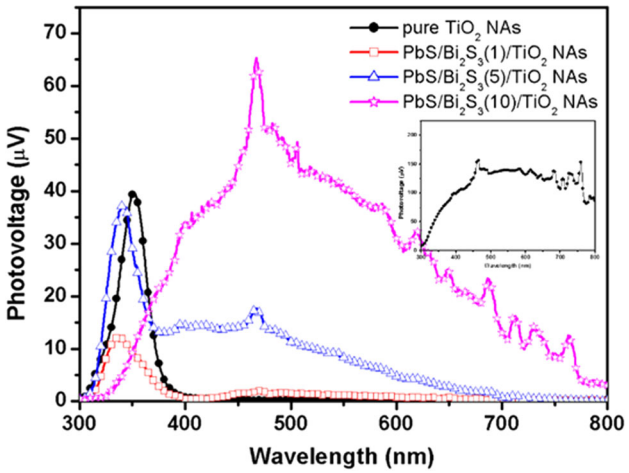

Fig. 5 Surface photovoltage (SPV) spectra of pure TiO_2 NAs and PbS/Bi_2S_3(n)/TiO_2 NAs (n = 1, 5, and 10, respectively), and pure Bi_2S_3 (*inset*)

The J–V and P–V characteristics of pure TiO_2 NAs and PbS/Bi_2S_3(n)/TiO_2 NAs electrodes in 0.5 mol L^{-1} Na_2S electrolyte are shown in Fig. 6a, b, respectively. And then, the corresponding parameters of photoelectrical performances are summarized in Table 1. The plain TiO_2 NAs electrode exhibits a negligible photoelectrical property. The short-circuit photocurrent (J_{sc}) and photo conversion efficiency (η) of plain TiO_2 NAs electrode are 1.01 mA/cm^2 and 0.26 %, respectively. For PbS/Bi_2S_3(n)/TiO_2 NA electrodes, the J_{sc} firstly increases and then decreases with the concentration of Bi^{3+} (n, n = 1, 5, and 10), reaching 2.88, 4.70, and 1.51 mA/cm^2, respectively. Accordingly, the highest η of 1.13 % is obtained from PbS/Bi_2S_3(5)/TiO_2 NAs electrode, which is around four times higher than that of plain TiO_2 NAs electrode. This result indicates that PbS and Bi_2S_3 nanoparticles co-sensitized on TiO_2 NAs can remarkably improve their photoelectric property.

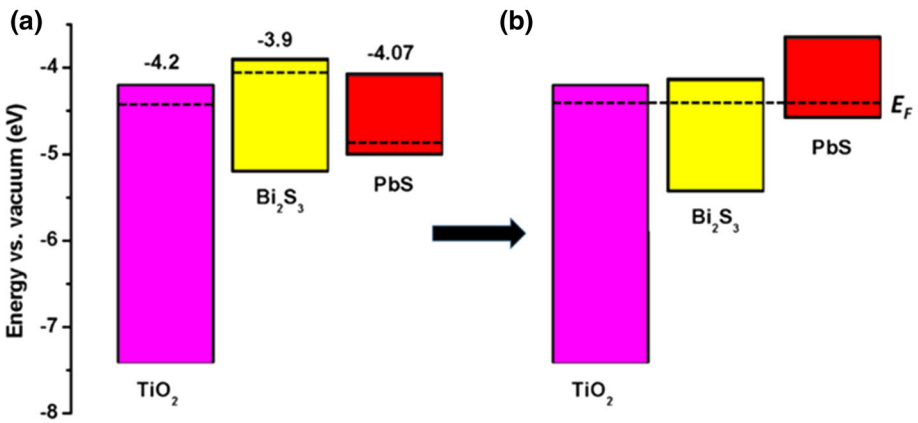

Fig. 4 Energy band diagram of PbS, Bi_2S_3, and TiO_2 before **a** and after **b** forming heterojunction. The *dotted lines* indicate the position of Fermi level

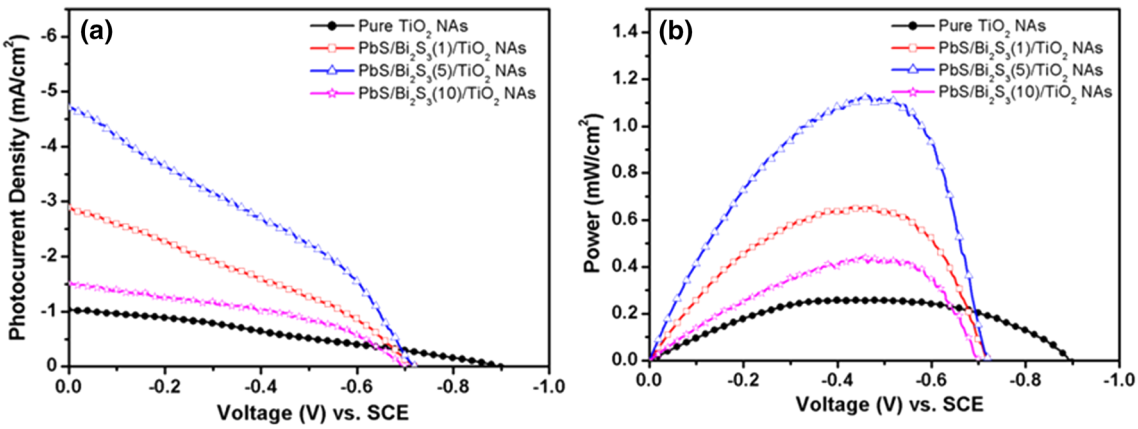

Fig. 6 *J–V* (a) and *P–V* (b) characteristics of pure TiO_2 NA and PbS/Bi_2S_3(*n*)/TiO_2 NA electrodes ($n = 1$, 5, and 10, respectively)

Table 1 Parameters of photoelectric property of TiO_2 NA and PbS/Bi_2S_3(*n*)/TiO_2 NA electrodes

Sample	J_{sc} (mA/cm^2)	V_{oc} (V)	*FF*	η (%)
Pure TiO_2 NAs	1.04	0.90	0.28	0.26
PbS/Bi_2S_3(1)/TiO_2 NAs	2.88	0.72	0.31	0.65
PbS/Bi_2S_3(5)/TiO_2 NAs	4.70	0.72	0.33	1.13
PbS/Bi_2S_3(10)/TiO_2 NAs	1.52	0.70	0.42	0.45

J_{sc}, V_{oc}, *FF*, and η are the short-circuit current density, open-circuit voltage, fill factor, and overall power conversion efficiency, respectively

The improved photoelectrical property of PbS/Bi_2S_3(*n*)/TiO_2 NAs electrodes may be attributed to several reasons. Firstly, the light response of TiO_2 NAs electrodes is extended from the UV to visible region after being co-sensitized by PbS and Bi_2S_3 NPs. This means that more sunlight can be used to generate the photocurrent. Secondly, as shown in Fig. 4b, Bi_2S_3/TiO_2 and PbS/Bi_2S_3/TiO_2 heterojunctions have been formed, and then the Fermi levels of TiO_2, Bi_2S_3, and PbS tend to reach balance, producing efficient charge transfer channel. Thirdly, the interfacial electric field in Bi_2S_3/TiO_2 and PbS/Bi_2S_3/TiO_2 heterojunction may prevent the recombination of photogenerated electron–hole pairs. However, higher concentration of Bi^{3+} would cause conglomeration of the crystal nucleus, and moreover, excess Bi_2S_3 would act as potential barrier for charge transfer. As a result, the photoelectric properties of PbS/Bi_2S_3(*n*)/TiO_2 NAs would not be further improved. The best photoelectrical performance is obtained from PbS/Bi_2S_3(5)/TiO_2 NAs electrode, in which J_{sc} and η are 4.70 mA/cm^2 and 1.13 %, respectively.

4 Conclusions

PbS/Bi_2S_3/TiO_2 NAs has been fabricated by a three-step process containing hydrothermal and sonication-assisted SILAR method. PbS NPs were attached to Bi_2S_3(*n*)/TiO_2 NAs, in which the size of PbS NPs was maintained lower than 4 nm by controlling the SILAR cycles. PbS and Bi_2S_3 NPs were co-sensitized on TiO_2 NAs to enhance their photoelectric property. When the concentration of Bi^{3+} was 5 mmol/L, the best photoelectric property was obtained. J_{sc} and η of PbS/Bi_2S_3(5)/TiO_2 NAs were respectively 4.70 mA/cm^2 and 1.13 % under an illumination of 100 mW/cm^2.

Acknowledgments The research was supported by Program of International S&T Cooperation (2013 DFA51050), National Magnetic Confinement Fusion Science Program (2013GB110001), the 863 Program (2014AA032701), the National Natural Science Foundation of China (11405138, 51302231), and the Western Superconducting Technologies Co., Ltd.

References

1. Slezak M (2013) Solar-powered cars streak across Australia in 3000 km race. New Sci 220(2939):19–20
2. Abbe G, Smith H (2016) Technological development trends in solar-powered aircraft systems. Renew Sust Energy Rev 60:770–783
3. O'regan B, Gratzel M (1991) A low-cost, high-efficiency solar cell based on dye-sensitized. Nature 353(6346):737–740
4. Kamat PV (2008) Quantum dot solar cells. Semiconductor nanocrystals as light harvesters. J Phys Chem C 112(48):18737–18753
5. Mali SS, Desai SK, Kalagi SS et al (2012) PbS quantum dot sensitized anatase TiO_2 nanocorals for quantum dot-sensitized solar cell applications. Dalton Trans 41(20):6130–6136
6. Cai FG, Yang F, Jia YF et al (2013) Bi_2S_3-modified TiO_2 nanotube arrays: easy fabrication of heterostructure and effective enhancement of photoelectrochemical property. J Mater Sci 48(17):6001–6007

7. Sun WT, Yu Y, Pan HY et al (2008) CdS quantum dots sensitized TiO_2 nanotube-array photoelectrodes. J Am Chem Soc 130(4):1124–1125
8. Gong D, Grimes CA, Varghese OK et al (2001) Titanium oxide nanotube arrays prepared by anodic oxidation. J Mater Res 16(12):3331–3334
9. Cai F, Yang F, Zhang Y et al (2014) PbS sensitized TiO_2 nanotube arrays with different sizes and filling degrees for enhancing photoelectrochemical properties. Phys Chem Chem Phys 16(43):23967–23974
10. Rath AK, Bernechea M, Martinez L et al (2012) Solution-processed inorganic bulk nano-heterojunctions and their application to solar cells. Nat Photon 6(8):529–534
11. Zhao Q, Wang D, Peng L et al (2007) Surface photovoltage study of photogenerated charges in ZnO nanorods array grown on ITO. Chem Phys Lett 434(1):96–100
12. Peter LM, Wijayantha KGU, Riley DJ et al (2003) Band-edge tuning in self-assembled layers of Bi_2S_3 nanoparticles used to photosensitize nanocrystalline TiO_2. J Phys Chem B 107(33): 8378–8381
13. Hyun BR, Zhong YW, Bartnik AC et al (2008) Electron injection from colloidal PbS quantum dots into titanium dioxide nanoparticles. ACS Nano 2(11):2206–2212
14. Pattantyus-Abraham AG, Kramer IJ, Barkhouse AR et al (2010) Depleted-heterojunction colloidal quantum dot solar cells. ACS Nano 4(6):3374–3380
15. Jiang J, Zhang X, Sun P et al (2011) ZnO/BiOI heterostructures: photoinduced charge-transfer property and enhanced visible-light photocatalytic activity. J Phys Chem C 115(42):20555–20564